ZESZYTY NAUKOWE POLITECHNIKI ŚLĄSKIEJ 2003
Seria: GÓRNICTWO z. 257 Nr kol. 1599

Stanisław F. ŚCIESZKA
Politechnika Śląska

TESTING MECHANICAL PROPERTIES OF MATERIALS FOR MINING TOOLS. ABRASIVE WEAR MEASUREMENT METHODS - A REVIEW

Summary. Techniques for wear resistance evaluation of materials for mining and drilling tools are extensively discussed in this paper. The integrated testing method based on edge chipping in granular abrasive medium is discribed.

BADANIA WŁASNOŚCI MECHANICZNYCH MATERIAŁÓW NA NARZĘDZIA GÓRNICZE. PRZEGLĄD METOD WYZNACZANIA ODPORNOŚCI NA ZUŻYWANIE ŚCIERNE

Streszczenie. Praca zawiera przegląd metod badania odporności na zużywanie ścierne materiałów stosowanych na ostrza narzędzi górniczych i wiertniczych. Opisano także zintegrowaną metodę łącznego badania odporności na kruche pękanie i odporności na zużywanie ścierne.

1. Introduction

Abrasive wear occurs when material is removed from the surface of a component by hard particles or hard protuberances that are forced against and move along the solid surface [1-5]. Several qualifying terms can be used in describing abrasion. A distinction is often made between two-body abrasive wear and three-body abrasive wear. Two-body abrasive wear is exemplified by the action of sand paper on a surface. Hard asperities or rigidly held grits pass over the surface like a cutting tool. In three-body abrasive wear, on the other hand, the grits are free to roll as well as slide over the surface, since they are not held rigidly. Abrasion is often further categorized as being low stress or high stress. Low-stress abrasion occurs when

the abrasive remains relatively intact. High-stress abrasion exists when abrasive particles are being crushed [4-6].

In real industrial situations a single mechanism only occurs rarely. This may be a case when the abrasion is an intended and controlled technological process in component manufacture, such as filing or grinding. In most industrial cases, however, abrasion occurs randomly in machine operation and is a mixed-mode type.

Every individual event of material removal from a surface during abrasion can be explained by several mechanisms [6, 7]. These mechanisms include plastic deformation, cutting, fracture, fatigue and melting.

The effect of abrasion is particularly evident in the industrial area of agriculture, mining, mineral processing and earth moving. In these areas the cost of abrasion is high and action which combats the wear is very important. The action may result in a machine component redesign, operational variables change or materials optimization. Materials optimization can only be done after the pragmatic ranking of various materials on laboratory tribotesters is completed.

A survey by the National Physical Laboratory in the UK identified over 400 wear testing standards in use around the world [5]. The likely reason that so many wear tests have been developed is that most of the tests have been developed either by investigators looking very fundamentally at the wear properties of materials, or by industries trying to reproduce the operating conditions in some particular application. The short review summarized in Figure 1 is restricted to only these tribotesters which are used for a laboratory simulation of the three-body type of abrasion particularly evident e.g. wherever minerals are handled. Figure 1 and references allow a comparison and are relating the novel, proposed method to other similar testing methods which are already well-established or standardized.

One of the advantages of the proposed method of testing is well-defined stress conditions within the bed of abradant and on the interface zone between the sample and the bed of abradant. These pressure conditions are controlled by normal force, P, and by shear strength of the abradant and are easy to alter by changing normal force (equations 1-3).

The attrition and comminution processes within shear zones together with a continual outflow of the already pulverized abradant to the upper part of the chamber through the gap between disc and cylinder were securing the presence of constantly changing layers of fresh and sharp abradant particles in the interface zone. This contributes towards an enhancement of the repeatability and reproducibility of the test results.

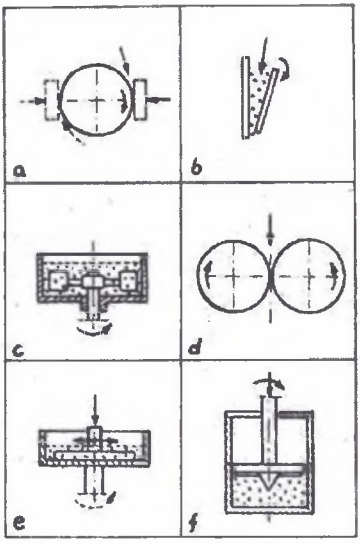

Fig. 1. Schematic illustration of dry and wet three-body abrasion testers: (a) rotating wheel (rubber or steel) and rotating ball abrasion testers – ASTM G65, ASTM B611, ISO 12962 and ASTM G105; (b) jaw crusher gauging tester – ASTM G81; (c) YGP abrasion tester [9] – BS 1016-111 and ISO 12900; (d) BCURA roll mill abrasion tester [10]; (e) reciprocating or rotating abrasion tester [8] – ASTM G75; (f) shearing blade abrasion tester – novel proposed tester

Rys. 1. Schematy testerów do badań zużycia ściernego: (a) obrotowy krążek lub kula – ASTM G65, ASTM B611, ISO 12962 i ASTM G105, (b) tester szczękowy – ASTM G81, (c) tester YGP [9] – BS 1016-111 oraz ISO 12900, (d) tester rolkowy BCURA [10], (e) tester o ruchu posuwisto-zwrotnym lub obrotowym [8] – ASTM G75, (f) proponowany nowy tester

Some disadvantages of the new method are related to the tester's geometrical constraints, e.g. to sensitivity of the comminution process to the gap change as experiments progress.

2. An integrated testing method based on in granular abrasive medium

The controlled conjoint action of a granular, hard abradant both as multipoint source of loading of the sample of hard material in the vicinity of edge and as hard, angular abradant can be used for ranking materials for both toughness and for wear resistance (Fig. 1f). This conjoint action takes place within a cylindrical chamber filled with granular abradant inside which normal stress, σ_n,

$$\sigma_n = \frac{P}{\pi R^2} \tag{1}$$

(where R is the internal radius of chamber) is controlled by external loading P. External torque, T, applied to the drive shaft is used to overcome the shear resistance of granular abradant.

$$\tau = \frac{3}{2}\frac{T}{\pi R^3} \tag{2}$$

The maximum shear resistance, τ for shearing a granular material, can also be expressed as

$$\tau = \sigma_n \tan\phi \tag{3}$$

It is widely accepted [2] that the shear resistance consists of the internal, frictional component between particles, which is a combination of rolling and sliding friction and an additional component arising from shearing against interlocked particles accompanied by particle crushing [1]. Equation (25) is one of the simplest formulas expressing $\tau - \sigma_n$ dependence in soil mechanics. For more general cases, in particular under a high normal stress (which is a typical for experiments analyzed here), this formula must be replaced by the relationship

$$\tau = C + \sigma_n \tan\phi \tag{4}$$

where C is called the cohesion.

The method which enables simultaneous brittle fracture and abrasion testing allows for simulation of stress and sliding speed conditions found e.g. between drills and rock. But in fact any material combination (i.e. material of bar-sample or granular abradant-mineral sample) can be used under any operating condition (i.e. normal stress, sliding velocity of temperature). Another advantage of the tribotester itself is that the ground abradant – granular mineral is allowed to leave the attrition area through the gap between a disc and a wall of the cylindrical chamber (Fig. 2), as occurs in actual drilling or grinding.

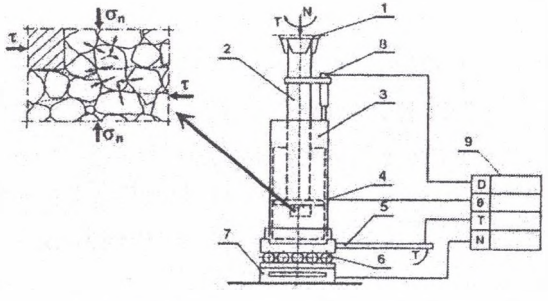

Fig. 2. Schematic diagram of apparatus, and interpretation of interaction between the particulate mineral and the bar within the shear zone: 1 - Drill chuck; 2 - Drive shaft; 3 - Cylindrical chamber; 4 - Thermocouple; 5 - Torque indicator; 6 - Thrust bearing; 7 - Force indicator; 8 - Displacement indicator; 9 - Recorder

Rys. 2. Schemat przyrządu badawczego: 1 - uchwyt, 2 - wał, 3 - cylindryczny pojemnik, 4 - termopara, 5 - czujnik momentu, 6 - łożysko osiowe, 7 - czujnik siły, 8 - czujnik przemieszczenia, 9 - drukarka

The apparatus consists of the disc rotating in the cylindrical chamber under normal force. The specimen bars are attached to the underside of the disc. The specimen bars are made from the materials (hardmetals, ceramics and cermets) being tested. The procedure diagram for the proposed optimal testing is shown in Figure 3.

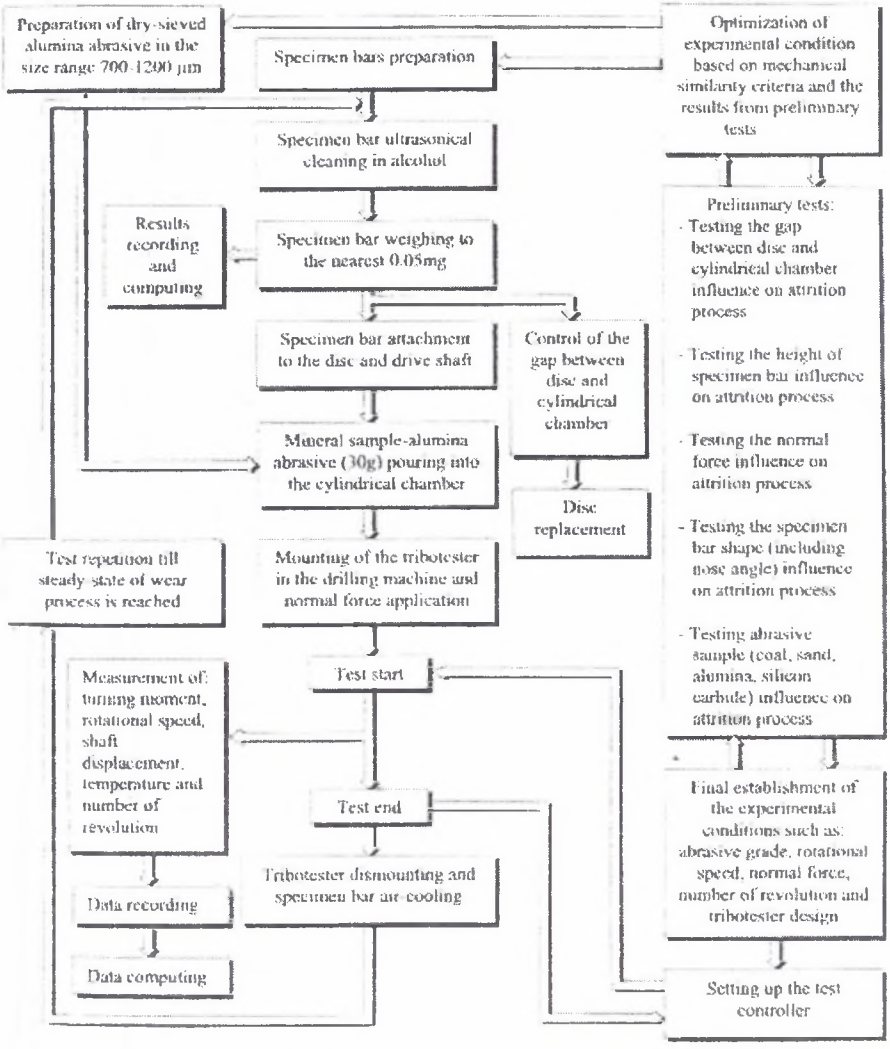

Fig. 3. Block diagram of test procedure and setting optimal design and operating parameters of a tribotester [1]
Rys. 3. Schemat blokowy procedury badań [1]

It is proposed to assemble the tribotester in the drilling machine (Fig. 4). A normal force should be applied in order to create the required stress between the specimen bar and the bed

of abradant-granular mineral. In fact the thickness of the granular abrasive layer should never be smaller than 20 mm. Every individual test should consist of a specified (optimal) number of revolutions, e.g. a set of 10 revolutions was recommended for alumina abradant (Fig. 5) and should be repeated ten times.

The results should be calculated using the following equations:

- The mass loss of the specimen-bar in mg is given by

$$\Delta m = m_1 - m_2, \tag{5}$$

where m_1 is the initial mass of the bar and m_2 is the final mass of the bar, mg.

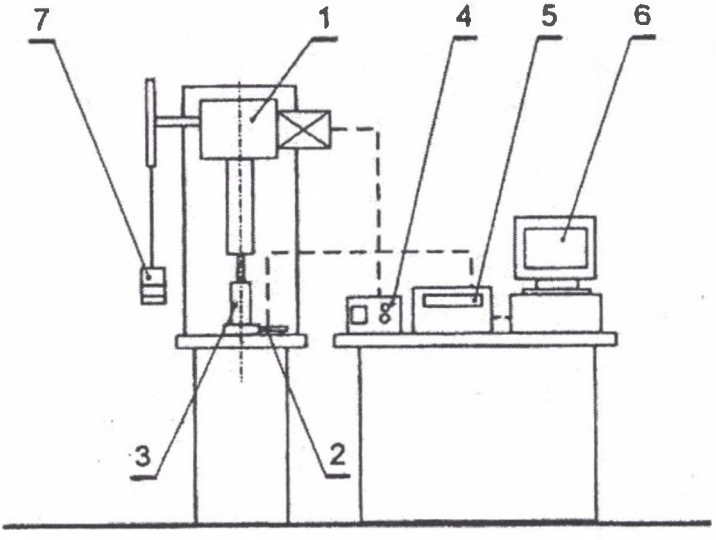

Fig. 4. Overall set-up of the tribotester: 1 - Upright drilling machine providing controlled rotary motion and normal loading to the drive shaft; 2 - Torque indicator; 3 - Cylindrical chamber and shaft of the tribotester; 4 - Test controller; 5 - Transducer and recorder; 6 - Computer data processing system; 7 - Load.

Rys. 4. Układ stanowiska pomiarowego: 1 - wiertarka, 2 - czujnik momentu, 3 - tribotester, 4 - sterownik, 5 - drukarka, 6 - komputerowy akwizytor danych, 7 - obciążenie

– W_v is the volumetric wear of the bar, mm^3

$$W_v = \frac{\Delta m}{\zeta}, \tag{6}$$

where ζ is the density, gcm^{-3}.

– $\overline{W}_v$ is the mean volumetric wear, mm^3. $\overline{W}_v$ is an arithmetic mean value of wear during the steady stage of wearing controlled by abrasive wear process (Fig. 5).

$$W_v = \frac{\sum W_v \, nkj}{nkj} \tag{7}$$

where n is the number of specimens per grade, k is the number of edges per specimen (3) and j is the number of repetitions (Fig. 5).

– WR is defined as wear resistance, mm^{-3},

$$WR = \frac{1}{W_v} \tag{8}$$

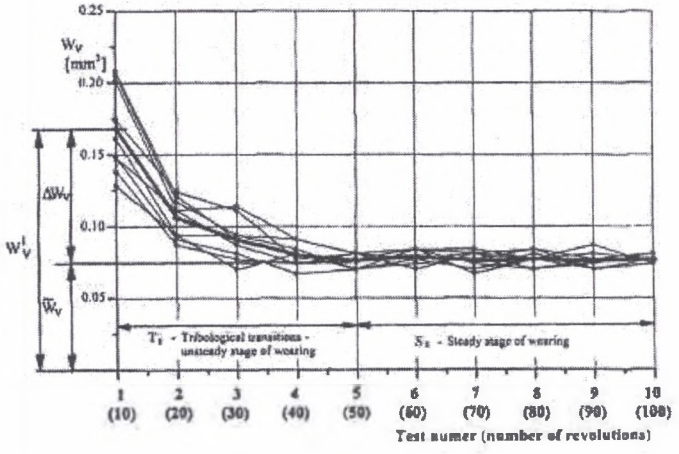

Fig. 5. Graphical interpretation of wear indicators such as W_v^1, ΔW_v and $\overline{W}_v$ based on experimental data with hardmetal tested with alumina as an abradant, where T_s is a tribological transition – unsteady stage of wear process controlled by brittle fracture and S_s is a steady stage of wear process controlled by abrasion

Rys. 5. Graficzna interpretacja wskaźników zużycia W_v^1, ΔW_v oraz $\overline{W}_v$ przy założeniu, że T_s jest okresem niestabilnego zużywania kontrolowanym przez pękanie krawędzi, a S_s jest okresem stabilnego zużywania ściernego

– WR_e is effective wear resistance, kJ mm^{-3},

$$WR_e = \frac{El}{W_v} 10^{-3} \tag{9}$$

where El is the energy input, $El = 2\pi Ti$, Nm.

T is the average integral value of torque (equations 1, 2, 3).

$$T = \frac{2}{3}\pi R^3 \tau = \frac{2}{3} PR \tan\phi \tag{10}$$

i is the number of revolutions

ϕ is the friction angle.

– ΔW_v is the initial increment of wear in mm^3,

$$\Delta W_v = W_v^1 - \overline{W}_v \tag{11}$$

where W_v^l is the mean volumetric wear for all tests number l with the given material grade (Fig. 5), then

$$W_v^l = \frac{\sum W_{vnk}^l}{nk} \tag{12}$$

– S is the equivalent fracture surface in mm^2 and is calculated from ΔW_v assuming that the crack surface produced during the test is flat and parallel to one side of the bar (prism), i.e.

$$S = \left(\frac{2\Delta W_v l}{\sin 60^\circ}\right)^{\frac{1}{2}} \tag{13}$$

where l is the length of the bar.

The procedure presented above is an integrated testing method for hard material abrasion resistance and fracture toughness evaluation is based on a concept of precise distinction between initial processes tribological transition (T_s) controlled by fracture edge damage and the steady stage of wearing (S_s) predominantly controlled by microabrasive wear mechanisms (Fig. 5).

The steady stage of wearing (S_s) yields a rating of the wear resistance of materials. In steady-state wear, the spread of results reported in previous investigations [1] was remarkably small, which when combined with the very accurate mass-loss measurement, makes the method very discriminating.

The method presented above does not produce the fracture toughness value (e.g. K_{IC}) as directly as the standardized plain strain fracture toughness tests does. The integrated testing method requires the theoretical or empirical models (formulae) which describe the relationship between fracture toughness and other mechanical properties. These formulae are usually based on well established assumptions and laws such as energy balance the Hertzian stress distribution, or on an empirical and semi-empirical relationships which were proved to be valid in the specified range [4, 6].

In accordance with the objectives of the present work showed in the introduction, the following formulae are proposed for further study and the least square fit evaluation:

(a) Relationship applied in previous investigations by Ścieszka and Filipowicz [1].

$$K_c = \beta\left(\frac{E}{H}\right)\left(\frac{1}{S}\right)(El \times P)^{\frac{1}{2}} \tag{14}$$

(b) Relationship based on Hornbogen study [3].

According to Hornbogen the transition from the unsteady to the steady stage of wear is equivalent to the change in probability of wear particle formation. This probability can be related to the plastic strain ε_p produced during an asperity interaction, and the critical strain ε_c,

at which cracks start to propagate in the material. In $\varepsilon_p > \varepsilon_c$ there is an increase probability of wear particle formation by fragmentation, hence wear rate depends on the fracture toughness and hence

$$K_c = \alpha\left(\frac{E^2}{H}\right)^{\frac{1}{4}}\left(\frac{1}{S}\right)^{\frac{1}{2}} p^{\frac{3}{4}} \tag{15}$$

(c) Relationship based on Hutchings study [4] on abrasive wear by brittle fracture which consists of the removal of material by lateral cracking. Hence

$$K_c = \gamma\left(\frac{E}{H}\right)^{2}\left(\frac{1}{S}\right)^{2}\left(\frac{1}{H}\right)^{\frac{5}{4}} p^{\frac{9}{4}} \tag{16}$$

(d) Relationship proposed by McCormick [23], equation (17)

$$K_c = \left(\frac{ME^2}{aH + bE}\right)^{\frac{1}{2}} \tag{17}$$

where $M = \frac{P_c}{d}$ is replaced by $M = \frac{El}{S}$ (equations 9 and 13) and is regarded to be equivalent to the concept introduced by McCormick of the edge toughness of the material. α, β, γ, a and b are the empirical constants which are computed using experimental results from tests (Fig. 3).

3. Abrasive wear and fracture mechanics in WC-Co hardmetals – a review

Because of their high hardness combined with some ductility, hardmetals find application where resistance to wear (abrasion or erosion) is an important consideration. Increasing the life of tools made from hardmetals, which is often limited by brittle failure, requires a full understanding of the mechanisms which are responsible for the macro-fracture of the tools and the abrasive wear of the hardmetals including individual WC grain micro-fracture and fragmentation.

The WC-Co structure contains a hard and brittle carbide phase, and a relatively soft and ductile binder, which is cobalt with dissolved carbon and tungsten. The formation of the real WC-Co structure is defined by the complex chemical and physical characteristics of the infiltrating phase and the chosen technological regime of the production. All these factors influence the final structure of hardmetal; size distribution of WC grains, distribution of Co binder, quality of grain boundaries, slip systems and all the defects such as dislocations, cracks, pores and their clusters, structural heterogeneities and inclusions [11, 12].

The wear resistance is obviously related to high hardness of WC grain in the structure combined with a small, but significant, level of ductility imparted by the cobalt binder. There is a certain level of interalloying between WC and cobalt which is sufficient to provide a strong interphase bond but not so great that phase dissolution or deterioration results.

The carbide grains are small and therefore they have good resistance to microfracture; nevertheless they do fracture [13]. In fact, according to Osburn [14], in rock cutting the predominant form of wear is through a mechanism of wear of micro-fracturing of surface layer. When the material is cooled from the liquid-phase sintering temperature the cobalt contracts more than the WC and this puts the more brittle WC grains under compressive stresses which further increases their resistance to brittle fracture [12].

Earlier studies [5-17] have shown that cemented carbides wear in abrasion conditions by different mechanisms and at different rates, depending on the relative hardness of the abrasive medium. For example, if the abrasive is more than 20 percent harder than the surface of the specimen, the material wear rate is relatively high, and material is removed from the alloy primarily by plastic extrusion from craters and grooves formed in the surface and by microfracture of the carbide skeleton [16]. Relatively "soft" abrasives, on the other hand, give a much reduced rate of wear and the mechanism appears to involve preferential binder removal followed by uprooting of carbide grains [17].

The mechanism of material removal in abrasion of WC-Co hardmetals by quartz according to Larsen-Basse [17] contains two distinct stages:

1. extrusion of cobalt binder metal due to repeated loading of the adjacent carbide grains by frictional shear forces followed by
2. cracking of the carbide grains and removal of the fragments by successive contacting abrasives; the propagation of the cracks is accelerated as the adjacent cobalt is extruded to the surface and the associated compressive stresses in the carbide grain are released. The WC grains break into small fragments and are gradually removed.

Larsen-Basse concluded [17] that the binder extrusion is the rate-controlling stage and the wear rate, therefore, is directed related to binder mean free path.

According to Blomberg et al [15, 16], during the rotary drilling of sandstone in regions where temperature exceeds 800 °C the chemical removal of the cobalt binder occurs as a result of reaction to form a cobalt silicate. Blomberg et al [15, 16] argued that preferential removal of cobalt from between the tungsten carbide grains was a result of the loose abrasive particles action. They pointed out that the abrasion on sandstone debris resulted in a rate of wear which was an order of magnitude greater than that during abrasion on the sandstone

block. Rapid and widespread selective removal of cobalt occurred from around the WC grains is followed by microspalling by the intergranular propagation of surface cracks. The removal of even a small amount of cobalt (0,2 μm in depth) from the surface e.g. by chemical etching renders the surface extremely susceptible to the propagation of intergranular cracking and microspalling during subsequent abrasion. Blomberg et al [15, 16] confirmed that the rate of wear of WC-Co hardmetals is controlled by the cobalt removal.

Cudden and Allen [18] examinations revealed that preferential removal of the binder occurs through two mechanisms namely abrasion and corrosion, which act synergistically. Cobalt is anodic to tungsten carbide and galvanic corrosion will take place when cemented carbides are subjected to a suitable electrolytic environment. The rate of corrosive attack is dependent on many factors such as the pH and electrolyte temperature and constitution. A low pH value leads to increased attack as does a rise in temperature.

The fracture process in WC-Co hardmetals has been the object of intensive research work [18, 20]. All models which try to relate toughness parameters (critical strain energy release rate, critical stress intensity factor) to microstructural parameters (carbide grain size, binder phase intercept length) suffer from over-simplified assumptions with respect to the details of crack propagation. Many of these models are logically based on observations of fracture surfaces which give information on the fracture path. Most models emphasize the role of plastic deformation in the binder phase because much of the final fracture occurs through the binder phase or at carbide binder interface. Recent results [21] show that the bridging mechanisms (Figure 6) behind the crack tip are the main fracture altering factors in the WC-Co systems. Fracture toughness of WC-Co systems with different microstructure parameters (volume fraction of binder – f_{Co}, mean grain size of WC grains – D_{WC}, mean free path in binder – L_{Co} and contiguity between WC grains – C_{WC}) are well described by means of two main parameters L_{Co} and C_{WC} using the relation:

$$K_{IC} = 19{,}24 + 5{,}61\, L_{Co} - 17{,}22\, C_{WC} \tag{18}$$

It seems that there are three main bridging mechanisms responsible for fracture toughness improvement in these systems:

(a) the ductile dimple failure of binder in the bridging zone behind the crack tip,

(b) the ductile dimple failure of the WC/Co boundary in the bridging zone associated with a small amount of WC/Co decohesion in the plane of the main crack,

(c) the ductile necking failure of binder associated with a strong WC/Co decohesion perpendicular to the plane of the main crack.

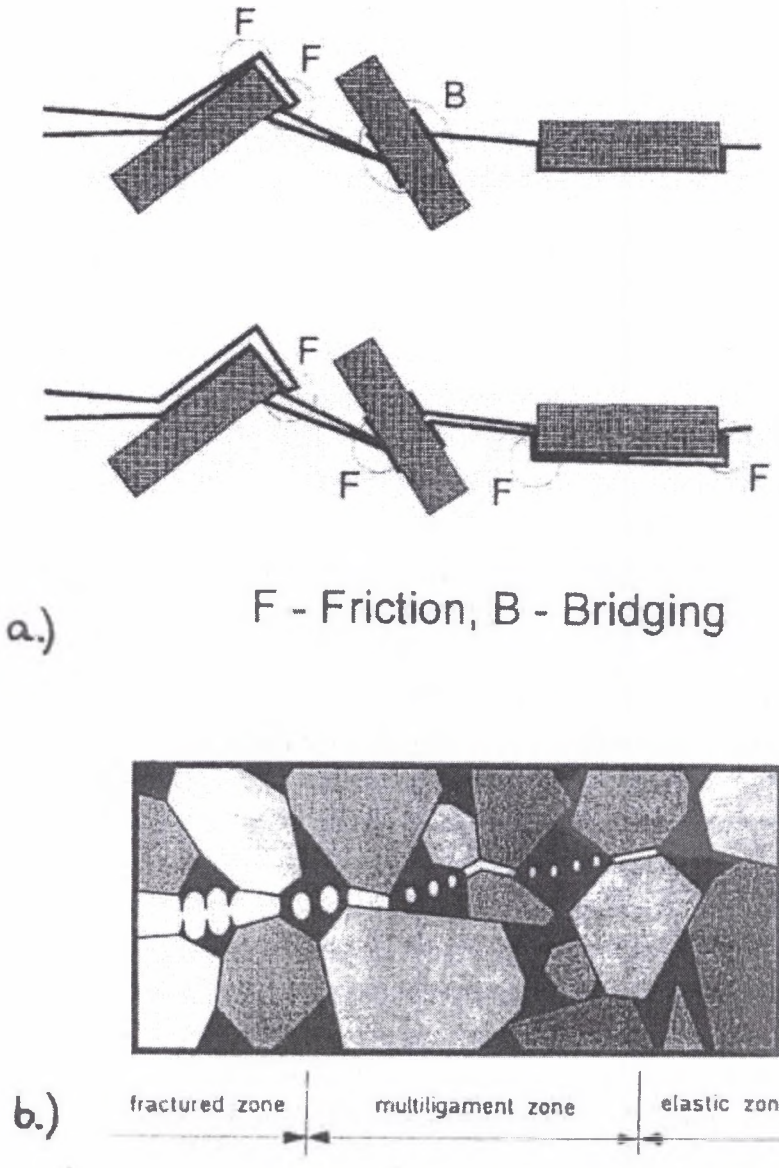

Fig. 6. Toughening mechanisms and fracture mechanisms [45,46] in polycrystalline brittle materials; (a) Main reinforcing mechanisms (frictional interlocking and crack bridging, (b) Crack tip region in a WC-Co alloy. At the right hand side the microstructure is still fully coherent and both phases are deformed elastically. In the multiligament zone crack path exists in the carbide skeleton while the binder ligament is deformed plastically by growth and coalescence of voids

Rys. 6. Mechanizm uplastyczniania i pękania [20, 21] kruchych polikrystalicznych materiałów: (a) główne mechanizmy wzmocnienia, (b) strefa czoła pęknięcia w węgliku spiekanym typu WC-Co

These mechanisms were detected with different frequencies of occurrence in WC-Co systems with different L_{Co} values.

Based on a large amount of fractographic work [13, 20, 21] the crack propagation in WC-Co alloys can be summarized by distinction of four types of fracture paths:

- Transgranular fracture through the binder phase
- Intergranular fracture along the carbide grain boundary
- Transgranular fracture through the carbide crystals

It is generally agreed that the main contribution to fracture energy comes from transgranular fracture through the binder phase. Nevertheless carbide fracture plays a decisive role since it precedes binder fracture and determines the direction (Figure 6) and the type of path in the binder or along carbide-binder boundary [20].

Since the crack to a large extent proceeds through the carbide phase, the contribution of this type of fracture must not be neglected in spite of its low specific fracture energy. In low cobalt alloys, this contribution amounts to 20% of the total fracture energy, and it still amounts to 5% in high cobalt alloys [20]. The fracture resistance of the carbide exerts a strong influence on the flow stress of the binder, this combined with the strong work-hardening of the cobalt binder, is thought to be the reason why the fracture toughness of WC-Co hardmetals is superior to that of other ductile phase reinforced ceramic matrix composites.

4. Stepwise abrasion tests

In order to avoid the situation that the heavily abraded surface displayed all stages of the wear process, making it difficult to distinguish and to identify the sequence of changes caused by abrasive action of abradant particles, stepwise tests were accomplished. The stepwise tests were carried out on the surface of hardmetal specimen grade ma11 (11wt%Co, hardness HV_{30} = 912 and the arithmetic mean linear intercept = 5,16 μm) which was polished to a fine metallographic finish and then abraded in steps. The tests consisted of six steps and were performed on the modified steel-wheel abrasion tester (Figure 1a) with silica abrasive wear process and to identify the sequence of micro-abrasion events. The wear surface after every step was examined by optical microscopy (OM) and by scanning electron microscopy (SEM).

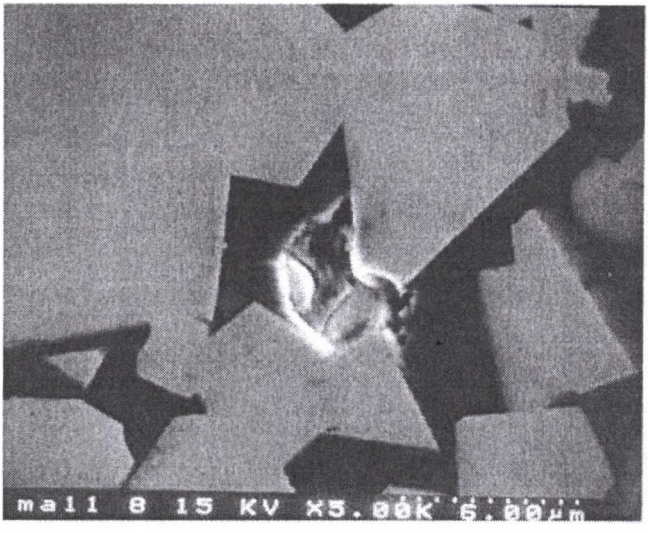

Fig. 7. SEM micrograph of the initial stage of wear associated with the pit formation as a result of mixed, transgranular and intergranular cracking modes induced by the forces between abrasive silica particles and the sharp corner of WC grain

Rys. 7. Obraz SEM wstępnej fazy zużycia (odprysku) wywołanego przez śródkrystaliczne i międzykrystaliczne pęknięcia

From the examination the two types of damage can be distinguished. The type of damage (termed type I) produced when the silica particle is trapped between the steel wheel and WC-Co specimen and resulting almost tangential impact creates the crater which encompasses about hundred WC grains. In this case the crater resembles that observed for the gouging scars and impact craters being characterized by appreciable plastic deformation [17]. The plastic deformation has mainly occurred in the binder phase. The WC grains remain relatively intact in the area where the silica particles were sliding over, or alternatively they were undergoing extensive cracking in these areas where the particles were forced to roll and finally were crushed. The type I of surface damage usually had linear dimension of 100 μm or more.

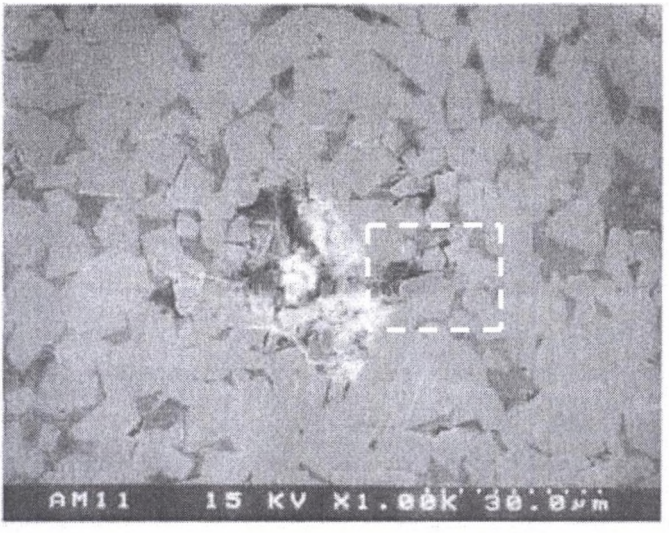

a)

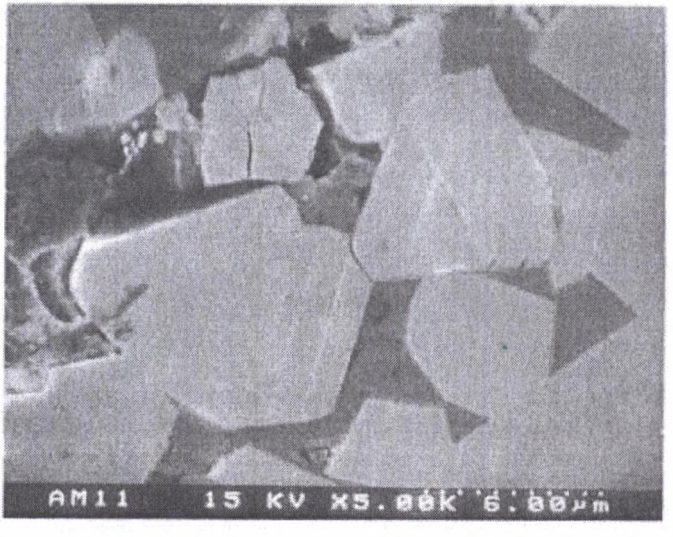

b)

Fig. 8. SEM micrograph of WC-Co surface showing localized but extensive surface damage after the second step of the abrasion test. This isolated pit formation (a) is typical for the early stage of wear. The pits are produced as a result of rapid selective cobalt removal and squeezed out of the surface by compressive stresses from around the tungsten carbide grains and consequent occurrence of microspalling of carbide grains by the propagation of surface cracks. The observation of the WC grains show the evidence of smearing of binder material and clear slip bands and cracking of WC grains (b)

Rys. 8. Obraz SEM powierzchni tarcia WC-Co z pojedynczym wgłębieniem (a) powstałego w wyniku selektywnego usuwania kobaltu oraz rozkruszania ziaren węglika WC

a)

b)

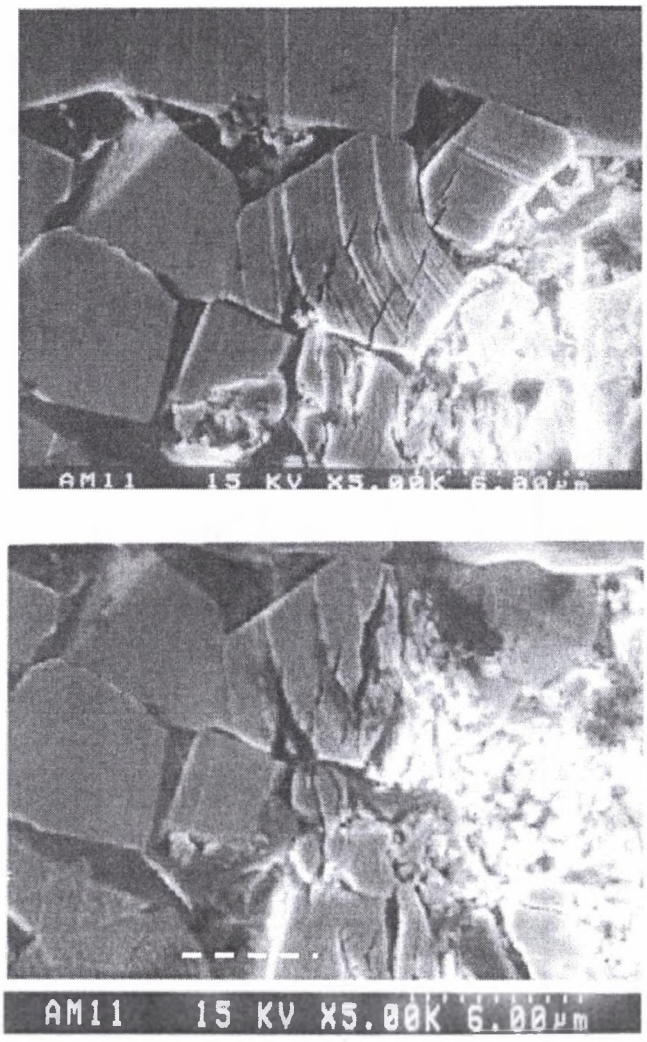

Fig. 9. SEM micrographs of WC-Co specimen after the second (a) and the fourth (b) steps showing a comparison between steps in two stages of abrasion. The initial stage-binder removal appears to be by small abradant particles and by extrusion. SEM micrographs clearly show cobalt smearing and consequently removal. The carbide grains show extensive deformation and cracking in step 2 which leads to the progressive fragmentation of the grains in the next steps. The wear fragments consist of minute (~0,2 µm) angular WC particles which are mixed with small Co particles and compacted in pits and cavities on the surface

Rys. 9. Obraz SEM powierzchni WC-Co po drugim (a) oraz czwartym (b) etapie zużywania. Widoczna jest stopniowa fragmentacja ziaren węglika wolframu

Figures 7 to 9 illustrate the type of damage (here termed type II) which occurred when the impact crater encompassed only a few (sometimes only one, as in Fig. 7) WC grains. Cracking and crushing of the brittle WC grains are evident e.g. Fig. 9. Debonding of the WC grains along their contiguous boundaries and at the cobalt matrix interface also occurred in

some cases. These damage features (i.e. cracking, crushing and debonding) occurred very frequently at the WC grain edges and corners, similar to the situations in Figures 8 and 9.

The stepwise abrasion test indicated that the two distinct types of behaviour occurred, namely type I which is produced by rounded (200-600 μm) and not crushed silica particles. The type I of damage is controlled by the particles compressive strength. This type resulted mainly from the plastic deformation of the binder but in the final stage when the abradant particle is crushed the massive WC grains crushing is generated. The second type of damage (type II) is produced by small, tough and already fragmented silica particles. This damage is formed mainly by the cracking of WC grains and is controlled by the WC grains fracture toughness.

5. Concluding remarks

Since the fracture toughness is often the major limiting parameter controlling the use of cermetals as drilling and cutting tools, there is a need for research aimed at increasing toughness without sacrificing wear resistance. To aid in this objective, a simple and reliable integrated testing method, in which a conjoint action involving both fracture and abrasion is needed for quick assessment of progress in such research. A broad survey on fracture toughness measurement methods, alternative techniques for fracture toughness evaluation and abrasive wear measurement methods indicate that the new integrated method based on the concept of edge chipping is particularly suitable for this application. Hard composite materials including hardmetals show both ductile and brittle materials behaviour with such microprocesses as plowing, cutting, microfatique, wedge formation and microcracking. Factors that affect the abrasive wear of these materials include the orientation, size, modulus of elasticity, relative hardness, and brittleness of the second phase. All there microprocesses and microstructure factors should be taken into consideration when abrasive wear resistance and fracture toughness are investigated. In this context the simultaneous abrasion and brittle fracture testing is particularly advantageous.

REFERENCES

1. Ścieszka S. F., Filipowicz K.: Materiały na narzędzia górnicze. Nowe trendy w technice badań. Wydawnictwo Politechniki Śląskiej, 2001, 1-106.
2. Oda M., Iwashita K.: Mechanics of Granular Materials. Balkema, Rotterdam 1999, 50-57.
3. Hornbogen E.: The role of fracture toughness in the wear of materials. Wear 33, 1975, 251-259.
4. Hutchings I. M.: Tribology, Friction and Wear of Engineering Materials. Arnold, London 1992, 153.
5. Neale M. J., Gee M.: Guide to Wear Problems and Testing for Industry. Professional Eng. Publ. London 2000, 31-92.
6. Stachowiak G. W., Batchelor A. W.: Engineering Tribology, Butterworth-Heinemann, Woburn 2001, 487-497.
7. Tylczak H.: Abrasive Wear, ASM Handbook, Vol 18, ASM International, 1992, 184-190.
8. Almond E., Lay L., Gee M.: Comparison of sliding and abrasive wear mechanisms in ceramics and cemented carbides, Science of Hard Materials, Almond E, Brookes C, and Warren R, (eds), A Hilger Ltd, Bristol 1986.
9. Yancey H., Geer M., Price J.: Transactions AIME Mining Eng, March, 1951, 262-268.
10. Spero C.: Review of test methods for abrasive wear in ore grinding, Wear 146, 1991.
11. Slasar M., Dusza J., Parilak L.: Micromechanics of fracture WC-Co hardmetals, Science of Hard Materials, Almond E, Brookes C and Warren R, (eds), A Hilger Ltd, Bristol 1986.
12. Larsen-Basse J.: Binder extrusion in sliding wear of WC-Co alloys, Wear 105, 1985, 247-256.
13. Rowcliffe D., Jayaram V., Hibbs M., Sinclair R.: Compression deformation and fracture in WC materials, Materials Science and Engineering, A105/106, 1988, 299-303.
14. Osburn H.: Wear of rock-cutting tools, Powder Metallurgy 12, 24, 1969, 471-502.
15. Blomberg R., Perrott C., Robinson P.: Similarities in the mechanisms of wear of tungsten carbide-cobalt tools in rock and metal cutting, Wear 27, 1974, 383-390.
16. Blomberg R, Perrott C., Robinson P.: Abrasive wear of tungsten carbide-cobalt composites, Wear mechanisms, Materials Science and Engineering, 13, 1974, 93-100.
17. Larsen-Basse J., Koyanagi E.: Abrasion of WC-Co alloys by quartz, J. of Lubrication Technology 101, 1979, 208-211.
18. Cuddon A., Allen C.: The wear of tungsten carbide-cobalt cemented carbides in a coal ash conditioner, Wear 153, 1992, 375-385.
19. Anand K., Conrad H.: Microstructure and scaling effects in the damage of WC-Co alloys by single impacts of hard particles, J. Materials Science 23, 1988, 2931-2942.
20. Sigl L., Exner H.: Experimental study of the mechanics of fracture in WC-Co alloys. Metallurgical Transactions 18, 1987, 1299-1308.
21. Dusza J.: Fractographic failure analysis of brittle materials, Int. J. of Materials and Product Technology 15, 2000, 292-355.
22. Zum Gahr K.H.: Microstructure and Wear of Materials, Elsevier, Amsterdam 1987, 80-336.
23. Mc Cornick N.J.: Edge flaking of brittle inaterials. PhD, NPL Teddington 1993, 12-264.

Recenzent: Prof. dr hab. inż. Walery Szuścik

Omówienie

Praca zawiera przegląd metod badania odporności na zużywanie ścierne materiałów stosowanych na ostrza narzędzi górniczych i wiertniczych. Opisano także zintegrowaną metodę łącznego badania odporności na kruche pękanie i odporności na zużywanie ścierne, która opiera się na koncepcji wykorzystania do tego celu łupliwości krawędziowej w środowisku ścierniwa zgranulowanego. Aparat badawczy, całkowite oprzyrządowanie tribotestera oraz schemat blokowy procedury badań zostały przedstawione na ilustracjach i opisane. Przedstawiono także przegląd literatury na temat mechanizmów zużywania i pękania węglików spiekanych WC-Co. Dodatkowo zaprezentowano wyniki badań własnych – etapowych w celu uzyskania pełnej ilustracji mechanizmów zużywania i pękania. W kontekście uzyskanych wyników, które potwierdziły kruchy, jak również plastyczny mechanizm zniszczeń, szczególnie przydatna powinna okazać się proponowana nowa metoda badań.